A Multi-Model Assessment of Future Projections of North Atlantic and European extratropical cyclones in the CMIP5 climate models

Giuseppe Zappa *

National Centre for Atmospheric Science, Department of Meteorology, University of Reading, Reading, UK

Len C. Shaffrey

National Centre for Atmospheric Science, Department of Meteorology, University of Reading, Reading, UK

Kevin I. Hodges

National Centre for Earth Observation, University of Reading, Reading, UK

Phil G. Sansom

Exeter Climate Systems, University of Exeter, Exeter, UK

David B. Stephenson

Exeter Climate Systems, University of Exeter, Exeter, UK

* *Corresponding author address:*

E-mail: g.zappa@reading.ac.uk

ABSTRACT

The response of North Atlantic and European extratropical cyclones to climate change is investigated in the climate models participating in CMIP5 (Fifth Coupled Model Intercomparison Project). In contrast to previous multi–model studies, a feature tracking algorithm is here applied to separately quantify the responses in both the number and the intensities of extratropical cyclones. The wind speed (dynamical intensity) and the precipitation (hydrological intensity) of cyclones are both investigated. Moreover, a statistical framework is employed to formally assess the uncertainties in the multi–model projections. Under the mid range RCP4.5 emission scenario, the DJF response is characterised by a tripolar pattern over Europe, with an increase in the number of cyclones in central Europe and a decreased number in the Norwegian sea and in the Mediterranean. The JJA response is characterised by a reduction in the number of North Atlantic cyclones along the southern flank of the stormtrack. The total number of cyclones decreases in both DJF (-4%) and JJA (-2%). By classifying cyclones according to their intensity, we find that there is a slight basin–wide reduction in the number of cyclones associated with strong winds, but an increase in those associated with strong precipitation. However, in DJF, an increase in the number and intensity of cyclones associated with strong wind speeds is found over the UK and central Europe. These results are confirmed under the high emission RCP8.5 scenario, where the signals tend to be larger. The sources of uncertainty in these projections are discussed.

1. Introduction

Extra–tropical cyclones can have a large socio–economic impacts. High winds and extreme precipitation from extratropical cyclones can result in windstorm damage, flooding and coastal storm surge (Della-Marta and Pinto 2009). Extratropical cyclones are also an important component of the mid-latitude water cycle (Hawcroft et al. 2012), providing fresh water for agriculture and society. Developing our knowledge of how extratropical cyclones might change in a warmer world is critical to understanding how societies may need to adapt to climate change.

The 4th Assessment Report (AR4) of the Intergovernamental Panel on Climate Change (IPCC) summarised that increasing greenhouse gases will lead to "a poleward shift of storm tracks in both hemispheres that is particularly evident in the SH, with greater storm activity at higher latitudes" (Meehl et al. 2007). There is evidence that this simple picture is not a good description of the response of the North Atlantic stormtrack. In winter, climate model simulations show an eastward extension of the stormtrack associated with an increased storminess over the UK and central Europe (Sinclair and Watterson 1999; Geng and Sugi 2003; Leckebusch and Ulbrich 2004; Pinto et al. 2007b; Bengtsson et al. 2006; Pinto et al. 2009; Catto et al. 2011). This could enhance the windstorm risk and the economic loss potential due to cyclone activity (Pinto et al. 2007a; Della-Marta and Pinto 2009). Climate models also show a future reduction in the number of Mediterranean cyclones (Bengtsson et al. 2006; Lionello and Giorgi 2007; Raible et al. 2010), which could increase the susceptibility of the region to droughts. However, the spread in the model responses appears to be large (Ulbrich et al. 2008, 2009; Harvey et al. 2012).

A source of uncertainty in the response of North Atlantic cyclones is given by the complex interaction between different physical drivers of change (Woollings 2010). Since extratropical cyclones grow as baroclinic instabilities organised along oceanic stormtracks (Hoskins and Valdes 1990), any change in the mean baroclinicity of the atmosphere or in the efficiency of baroclinic conversion will likely affect cyclone behaviour (O'Gorman 2010). The future

increase in the atmospheric moisture content is a major driver of changes (Schneider et al. 2010). Increased latent heat release in the warm sector of cyclones might enhance cyclone development by generating additional available potential energy (Laîné et al. 2009). However, the increased poleward and upward moisture fluxes will also tend to reduce the zonal mean baroclinicity so that cyclone development might be instead inhibited (Held 1993). The polar amplification of global warming (Hwang et al. 2011), the expansion of the tropics (Fu et al. 2006) and the weakening of the Meridional Overturning Circulation (MOC) will further affect the baroclinicity of the North Atlantic region (Woollings et al. 2012).

As extratropical cyclones are complex dynamical features, their diverse behaviour is best analysed by tracking the individual trajectories using objective feature tracking algorithms. This allows the climate change response in the number and the intensities of cyclones to be quantified separately. However, due to the lack of high frequency data, cyclone tracking could not be applied to analyse earlier multi–model dataset, such as those provided in CMIP3 (the Third Coupled Model Intercomparison Project). Emerging pictures in the stormtracks' response to climate change, such as the one given in the AR4, have been built on the existence of consistent responses in single–model studies based on tracking algorithms (Schubert et al. 1998; Geng and Sugi 2003; Leckebusch and Ulbrich 2004; Bengtsson et al. 2006; Pinto et al. 2009; Catto et al. 2011) and on the results of multi–model analyses based on simple measures of stormtrack activity. This includes Eulerian bandpass filter variance statistics (Yin 2005; Ulbrich et al. 2008; O'Gorman 2010) and simple cyclone identification techniques (Lambert and Fyfe 2006). These approaches have limitations. The insight from the comparison of single–model studies is limited by the use of different tracking algorithms and metrics of cyclone intensity, which might highlight different aspects of cyclone behaviour. The Eulerian measures of stormtrack activity cannot discriminate between the changes in the number and in the intensity of cyclones, and provide no direct information on the response of the extremes of cyclone intensity.

The aim of this study is to assess the projections of North Atlantic and European cyclones

by investigating the climate change response of the CMIP5 models (Fifth Coupled Model Intercomparison Project, Taylor et al. (2012)). As high frequency data (6 hourly) is included for the first time in CMIP5, a cyclone tracking algorithm (Hodges 1994, 1995, 1999) can be used to quantify the future changes in the number, the dynamical intensity (wind speed) and the hydrological intensity (precipitation) of cyclones in a wide range of models. Moreover, a statistical framework is adopted to quantify the uncertainties in the model responses (Sansom et al. 2012). Both the boreal winter (DJF) and summer (JJA), which has been previously given little attention, are investigated.

The structure of the paper is as follows. The dataset, the tracking algorithm and the statistical framework are described in section 2. The future changes in the mean storminess are presented in section 3. Section 4 examines the future changes in the cyclones of strong intensity. Section 5 discusses the relation with the large scale state of the atmosphere and ocean. The conclusions of the study are presented in section 6.

2. Data and Methods

a. CMIP5 models

The climate change response of 19 CMIP5 models is determined by comparing thirty year periods of the HISTORICAL (1976–2005) present day simulations and the future climate simulations (2070-2099) forced by the Representative Concentration Pathway 4.5 (RCP4.5) and 8.5 (RCP8.5) scenarios (Taylor et al. 2012). In the HISTORICAL (HIST) simulations the CMIP5 coupled climate models are forced by the observed GHG concentrations, ozone, solar forcing, land use and aerosols over the last 150 years. The RCP4.5 simulations are future scenarios conditional on a midrange mitigation of GHG emissions. In particular, CO2 emissions peak by 2040 and progressively decline so that CO2 concentrations are stabilised at 543 ppm by 2100. This roughly corresponds to a doubling of CO2 concentration respect to pre–industrial conditions. High GHG emissions are instead specified in the RCP8.5 scenario,

where CO2 concentrations do not stabilise within the 21st century (Meinshausen et al. 2011).

The 19 CMIP5 models considered in this study are listed in table 1, including their horizontal and vertical resolutions and the number of analysed runs of the HIST and RCP ensemble simulations.

b. Cyclone tracking and data

Cyclones are identified and tracked using the Hodges (1994, 1995, 1999) objective feature tracking algorithm. This algorithm has already been applied to study the future response of extratropical cyclones in single model studies (Bengtsson et al. 2006, 2009; Catto et al. 2011). The main characteristics of the tracking algorithm are as follows. The 850 hPa vorticity is computed from the 6 hourly zonal and meridional wind speeds and it is then smoothed on a T42 grid by removing the spectral components of total wavenumber larger than 42 and smaller than 6. This procedure filters the small scale noise and the large scale background field. Cyclones are then identified as relative maxima in the filtered vorticity that exceed an intensity of $10^{-5}\,\mathrm{s}^{-1}$. The T42 smoothing also allows cyclones of similar spatial scales to be identified in models of different atmospheric resolutions (Blender and Schubert 2000). Once the vorticity maxima are identified, their tracks are determined by minimising a cost function for the track smoothness, measured as changes in direction and speed, subject to constraint on displacement and track smoothness. Finally, to avoid the inclusion of unrealistic stationary and short lived features, only the cyclone tracks that have a lifetime greater than 2 days and propagation greater than 1000 Km are retained for the analysis.

Both the dynamical and the hydrological intensity of cyclones are evaluated. The dynamical intensity of cyclones is measured by referencing the tracks to the full resolution maximum wind speed at 850 hPa searched within a five degree spherical cap centered on the T42 vorticity maxima. The cyclone hydrological intensity is measured by the 6 hourly precipitation rate averaged over the same five degree spherical cap. The 6 hourly precipitation rate, which

is not a standard CMIP5 diagnostic, is obtained by averaging the 3 hourly precipitation rate at the times leading and following the one of vorticity estimation. The choice of these metrics is also motivated from an impact assessment perspective, as winds and precipitation are strongly related to windstorms and floods. The sensitivity of the results to other metrics of dynamical intensity — minimum MSLP and maximum T42 vorticity at 850 hPa — has been tested and it is briefly discussed in section 4a. The spatial maps of the number of cyclones per month per unit area — i.e. the track density — and of the mean precipitation and wind speeds associated with cyclones are computed using the spherical kernel estimators described in Hodges (1996). The cyclone hydrological intensity in the RCP scenarios is only evaluated for an 18 years period (2082-2099), due to data availability.

c. Statistical framework

In this study, the mean climate response (β) is estimated from the unweighted multi–model mean of the difference between the historical and future day simulations. If available, multiple runs from each model are first averaged for each scenario. Sansom et al. (2012) showed that β is equivalent to the maximum likelihood estimate of the expected climate response from a two way ANalysis Of VAriance (ANOVA) framework (See the Appendix). We use this statistical framework to evaluate the statistical significance of the mean climate response and to compare the size of the mean climate response against internal variability (signal to noise ratio). Internal variability is here defined as the sampling uncertainty in the thirty-year means that is induced by aleatoric weather variations.

Consensus in multi–model projections is often evaluated by the sign agreement in the climate responses, or by comparing the size of the mean climate response against the spread of the model responses. These approaches tend to systematically reject consensus where the mean climate response is small compared to the internal variability (i.e. in regions of low signal to noise). However, additional information can be gained from a statistical analysis in regions of small mean climate response if climate models agree that the response is small.

To quantify this, we use the ANOVA framework to determine the uncertainty in the mean climate response from the differences in the responses of the models, which is called the *model–dependent* climate change component by Sansom et al. (2012), and from internal variability. If the mean climate response is small (i.e. in regions of low signal to noise) and the variance ratio (f^2) of the *model–dependent* component over the internal variability component $f^2 < 1$ then there is consensus between the models that the mean climate response is small. As the responses of the cyclone tracks have in general low signal to noise ratio (see section 3), the choice of this metric seems to be appropriate for this study.

3. Future response of the mean storminess

In this section we discuss the projected response of North Atlantic and European extratropical cyclones to climate change in the CMIP5 climate models. We begin by recapping the results of Zappa et al. (2012) who investigated the biases of the CMIP5 historical simulations against observations. The DJF and JJA mean climate change responses in the CMIP5 models (RCP4.5 - HIST) is then presented for the track density and intensity of North Atlantic cyclones. The individual model track density responses can be found in the supplementary material. Finally, the sensitivity of the climate change response in the RCP8.5 scenario is discussed.

a. The ability of the CMIP5 models to represent North Atlantic and European cyclones

In this subsection we present the biases of CMIP5 historical simulations against observations. The discussion of the model biases is brief and the reader can refer to Zappa et al. (2012) for more detail.

Figs. 1a,c show the DJF track density from ERA–Interim reanalysis (1980–2009) and the mean bias of the CMIP5 models (HIST - ERA–Interim). CMIP5 models tend to underestimate track density in the Norwegian sea and to overestimate it in a zonal band between the

subtropical Atlantic and central Europe. The magnitude of the biases are of the order of the 10–30% ERA–Interim values, and they show that the simulated North Atlantic storm-track is on average southward displaced in the Atlantic and too zonal into Europe. In the Mediterranean area too many cyclones tend to propagate north–east relative to the Alps, and a too few number propagates south–east along the Mediterranean sea. However, the CMIP5 models differ in the extent that they can capture the observed spatial distribution of cyclones. In particular, Zappa et al. (2012) shows that three models stand out in their ability to represent the position of the North Atlantic stormtrack and the number and intensity of North Atlantic cyclones.

Fig. 1d shows the bias in JJA track density bias of the CMIP5 models (HIST - ERA–Interim) is smaller compared to that found in DJF. As discussed in Zappa et al. (2012), the CMIP5 models are better at capturing the location and the tilt of the North Atlantic storm-track in JJA. However, some models tend to underestimate the total number of cyclones, which is associated with the mean track density bias found in Fig. 1d. The Mediterranean stormtrack shows weaker activity in JJA than in DJF in both the ERA–Interim reanalysis and in the CMIP5 models.

b. Winter, track density response

We now describe the mean DJF CMIP5 track density response to climate change for the RCP4.5 scenario. Fig. 2a shows the mean climate response (shading) and the mean state in the HIST simulations (contours). Moreover, Fig. 2b shows the statistical analysis based on the Sansom et al. (2012) statistical framework. The shading identifies the regions where the mean climate response is statistically different from zero at the 5% level. The colour of the shading gives the signal to noise ratio (β/σ). Black stippling identifies areas with consensus on the responses of the models ($f^2 < 1$).

The response in DJF track density over Europe is dominated by a tripolar pattern. There is a reduction in track density in the Norwegian sea and in the Mediterranean and

subtropical central Atlantic, while the track density increases close to the British Isles. The overall track density response over the North Atlantic suggests a reduction in the tilt of the North Atlantic stormtrack, and of an eastward extension of the stormtrack into Europe. This is consistent with the increase in the East Atlantic stormtrack activity found by Ulbrich et al. (2008) in the CMIP3 models. The mean track density response also resembles what found in some previous single–model studies (Sinclair and Watterson 1999; Geng and Sugi 2003; Leckebusch and Ulbrich 2004; Pinto et al. 2007b; Bengtsson et al. 2006; Pinto et al. 2009; Catto et al. 2011).

The analysis based on Sansom et al. (2012) statistical framework shows that the above described responses are all statistically significant at the 5% level (Fig. 2b). The signal to noise ratio is typically of the order of one, with larger values being found in the Mediterranean and smaller over the British Isles. Consensus in the responses of CMIP5 models is found over most of the domain. This includes region of low signal to noise ratio, which suggests that CMIP5 models agree that little track density change will occur in the west Atlantic and North America.

As described above, the most prominent spatial DJF biases in the CMIP5 models is a tendency to poorly capture the south–west to north–east tilt of the North Atlantic storm-track. The DJF response of the CMIP5 models in DJF can also primarily be interpreted as a change in the tilt of the stormtrack. This raises a number of questions concerning the sensitivity of the climate change response of North Atlantic cyclones to the historical biases in the CMIP5 climate models. To explore the robustness of the results relative to the historical biases, Fig. 3 shows the mean track density response computed for the CMIP5 models which, as described in Zappa et al. (2012), have a better representation of the stormtrack position and tilt: HadGEM2–ES, HadGEM2–CC[1], EC–EARTH and MRI-CGCM3. The response of this subset of models is similar to the mean CMIP5 response. In particular, the tripolar pattern is still identified and the track density still increases in the UK region and decreases

[1]This model, not included in Zappa et al. (2012), has cyclone statistics very similar to HadGEM2–ES

in the Norwegian sea. Therefore, the broad features of the North Atlantic response appear to be weakly sensitive to the historical biases.

c. Winter, cyclone intensity response

Figs. 2c–d show the change in the mean cyclones dynamical intensity (as measured by the 850 hPa winds) for the RCP4.5 scenario. The CMIP5 models show a statistically significant reduction in the dynamical intensity of cyclones over the Mediterranean, the subtropical Atlantic and the Norwegian sea. A slight increase is found in Northern France and Germany. Note that the mean response in the dynamical intensity of cyclones (Fig. 2c) and in the track density (Fig. 2a) tend to be spatially coherent and have the same sign: e.g. both the number and the dynamical intensity of cyclones decrease in the Mediterranean, and both show an increase close to the British Isles. Despite being significant, these signals have small signal to noise ratio. Consensus in the model responses is generally found. These results are consistent with the single model studies of Bengtsson et al. (2006); Pinto et al. (2007b).

Fig. 2e–f shows the future response in the mean precipitation associated with cyclones (hydrological intensity). The increase in the hydrological intensity is expected in response to the increased atmospheric moisture content in a warmer climate (Held and Soden 2006; Pall et al. 2007; Schneider et al. 2010). However, the response is not spatially uniform. The maximum increase occurs close to the east coast of the US, which corresponds with the region of maximum precipitation in the HIST simulations. The response is instead small, and not significant, in the oceanic region South East of Greenland. This pattern is consistent with the spatial distribution of the near surface atmospheric warming (see Fig. 9a).

The response in the mean hydrological intensity is also small in the Mediterranean area. This may be a consequence of the reduction in the dynamical intensity of cyclones which, by weakening the atmospheric vertical motions, tend to offset the thermodynamic tendency toward more precipitation (Emori and Brown 2005; Finnis et al. 2007). We cannot test the f^2 metric of consensus as the hydrological intensity is computed for a different number of

years in the HIST (1975–2005) and RCP4.5 (2082–2099) simulations. However, we find that more than 80% of the models tend to agree on the sign of the response in the areas with signal to noise ratio larger than two. The data limitation in the RCP4.5 scenario has less impact for the other statistical analyses.

In conclusion, there is emerging consensus in the response of North Atlantic cyclones in CMIP5 models. Rather than a poleward shift, the response is characterised by a tripolar pattern over Europe, with a reduction in cyclone activity (number and intensity) on both the northward and southward flank of the stormtrack and an eastward extension towards the British Isles. North of 45N and over the continents, the response of largest signal to noise is the increase in the mean hydrological intensity of cyclones. Instead, south of 45N, and especially in the Mediterranean, the track density reduction has the largest signal to noise. The mean dynamical intensity of cyclones tends to decrease apart from over central Europe, where there is a small, but significant, increase.

d. Summer, track density response

Fig. 4a–b shows the JJA CMIP5 track density response to climate change for the RCP4.5 scenario. The mean response to climate change is a reduction in track density on the southern flank of the stormtrack (35N–45N) and an increase in track density downstream of the southern tip of Greenland (∼60N). The pattern is consistent with the track density response found in single model studies (Geng and Sugi 2003; Bengtsson et al. 2006) and also with the transient eddy kinetic energy response found by O'Gorman (2010) in the CMIP3 models. Such a meridional dipole might be suggestive of a poleward shift of the stormtrack, and, as discussed in section 5, a poleward shift is effectively found in the upper tropospheric jet. However, at the surface, the reduction in the number of cyclones on the southern flank of the stormtrack seems to dominate. Also in JJA, as in DJF, the signal to noise of the responses is approximately one.

There is consensus in the track density responses of CMIP5 models over most of the North

Atlantic and Europe. No consensus is found in the reduction in track density over the United States and in the increase in track density close to Greenland. However, in North America the response has the same sign in the majority (>80%) of CMIP5 models, which suggests that a similar climate process, but of different magnitudes, is occurring in the different models. This uncertainty does not appear to be related with the HIST track density biases in the region. No consensus in the sign of the response is found in the track density increase close to Greenland. Differences in the representation of Greenland's orography and of its interaction with the response of the jet (see section 5) might contribute to such uncertainty.

e. Summer, cyclone intensity response

Fig. 4c–d shows that the mean dynamical intensity of cyclones decreases in JJA over the North Atlantic and North America, while no significant changes occur in the Norwegian sea. In particular, the signal is largest along the southern flank of the stormtrack, in correspondence with the region where track density also tends to decrease. Consistent with the track density response, consensus in the model responses is again found over most of the domain with the exception of North America. The reduction in the mean dynamical intensity of cyclones in JJA tends to be larger compared with that found in DJF.

Fig. 4e–f shows that the hydrological intensity of cyclones (precipitation) is projected to increase, especially over land north of 50N. The response is instead weak in the subtropical central and east Atlantic, where the hydrological intensity even tends to decrease locally. As discussed for the Mediterranean area in DJF, this suggests that the reduction in the dynamical intensity of cyclones in the subtropical Atlantic acts against the precipitation increase expected due the increased atmospheric moisture content. The signals are still large compared with internal variability, especially over land and North of 50N.

In conclusion, the future response of North Atlantic cyclones in JJA is characterised by a reduction in cyclone activity (number and dynamical intensity) on the southern flank of the stormtrack (30N–45N). At the same time there is an increase in the hydrological intensity of

cyclones especially over land and north of 50N. By comparing the signal to noise ratios, the increase in the precipitation of cyclones is the dominant signal emerging at high latitudes, while over a large mid–latitude area (30N–45N) it is the reduction in cyclone number and intensity that have the largest signal to noise ratio. Cyclone intensity and number are also predicted to decrease over North America, but the size of the response is more uncertain.

f. Sensitivity to scenario

Fig. 5a–b shows the DJF and JJA mean track density responses for the RCP8.5 scenario (RCP8.5-HIST). The patterns are very similar to those seen in the RCP4.5 scenario except the magnitude of the RCP8.5 responses is roughly double those in the RCP4.5 scenario, consistent with the increased anthropogenic forcing. The signal-to-noise is also larger. For example, the track density reduction on the southern flank of the stormtrack reaches signal to noise of about three in both DJF and JJA (not shown).

Table 2 summaries the sensitivity of the mean response to the emission scenario for different areas of interest. In particular, the mean response in the track density and in the dynamical and hydrological intensities area–averaged over Central Europe (20W–30E; 50N–60N) and the Mediterranean (10W–40E; 30N–45N) are presented for the RCP4.5 and RCP8.5 emission scenarios (these areas are also shown by boxes in Fig. 1a–b). The Mediterranean is only considered in DJF, when the regional stormtrack is more active. The 90% confidence intervals on the mean response are indicated.

For the RCP8.5 scenario, in the multi model mean, a very large track density response is found in the Mediterranean in DJF ($-20 \pm 2\,\%$). For the same scenario, the track density decreases over Central Europe in JJA (-10±2 %), but increases in DJF (4±1 %). The increase in the Central European track density is also associated with an increase in the mean dynamical intensity of cyclones (0.9±0.5 %). A large increase in the hydrological intensity of cyclones is also found over Central Europe in both DJF (18±1 %) and JJA (9±1 %).

4. Response of strong cyclones

We now describe the response of cyclones associated with strong wind speeds and precipitation. The response is presented using both basin–wide statistics, to determine the changes in the overall characteristics of the stormtrack, and as a function of the location, which is more appropriate for interpreting the regional impacts.

a. Basin–wide response

North Atlantic and European cyclones are defined as those reaching their maximum T42 vorticity at 850 hPa (the tracked variable) within 30N–90N and 80W–40E (the area is delimited in Fig. 1a–b). The frequency distribution (FD) of the maximum along–track dynamical intensity of North Atlantic and European cyclones, as measured by wind speed at 850 hPa, is then computed for each model. The multi–model mean of the FDs in the HIST and in the RCP4.5 simulations are shown in Fig. 6a–b. Little change is found between the two simulations. However, by looking at the difference (RCP4.5 - HIST) in the FDs we find a reduction in the number of cyclones associated with 850 hPa wind speed larger than 25 $\mathrm{m\,s^{-1}}$ in DJF and of 20 $\mathrm{m\,s^{-1}}$ in JJA. This signal can also be seen in the tail of the FD, suggesting that the basin–wide response is a reduction in the number of cyclones associated with strong 850 hPa wind speeds.

To better compare the CMIP5 models, a metric of the number of strong cyclones is introduced which takes into account the HIST biases of the models. Strong cyclones are defined as those exceeding a threshold in the maximum along–track wind speed at 850 hPa. For each model and season, the threshold is chosen to be equal to the 90th percentile of the maximum along–track wind speed FD of North Atlantic and European cyclones in the HIST simulation. This allows us to always consider the top 10% strongest cyclones relative to the model climatology. In the multi–model mean, the number of strong North Atlantic cyclones decreases of $-8 \pm 3\,\%$ in DJF and of $-6 \pm 3\,\%$ in JJA. Moreover, the total number of North

Atlantic cyclones decreases of $-3.6 \pm 0.6\,\%$ in DJF and of $-1.9 \pm 0.6\,\%$ in JJA.

Fig. 7a–b shows the distribution of the CMIP5 model responses in the total number of cyclones, and in the number of cyclones associated with strong wind speeds, so that the spread of the responses can be investigated. The responses are shown for both the RCP4.5 and RCP8.5 scenarios. The total number of cyclones decreases in the majority of CMIP5 models in both the seasons and scenarios, i.e. the interquartile ranges lie entirely below zero. However, the spread of the model responses in JJA is roughly the double than in DJF, thus suggesting larger uncertainty in the summer. A similar picture is found for the response in the number of strong cyclones: a reduction is found in the majority of models in both DJF and JJA, but larger uncertainty characterises JJA.

In summary, we have found that both the total number of North Atlantic cyclones and those of strong dynamical intensity tend to decrease in response to climate change. The sensitivity of the results to the adopted metric of cyclone dynamical intensity has been tested. We find that CMIP5 models also show a reduction in the number of North Atlantic cyclones associated with strong T42 vorticity at 850 hPa. When considering the along–track minimum in MSLP, the number of deep cyclones tend to decrease in DJF but a slight increase, with large spread, is found in JJA. This highlights that care is needed when using MSLP to evaluate changes in dynamical intensity under climate change. The minima in MSLP can be also affected by the variations in the large scale MSLP field (Bengtsson et al. 2009; Ulbrich et al. 2009). Moreover, as the radius of cyclones also tend to increase, deeper cyclones might not imply stronger wind speeds (Schneidereit et al. 2010).

The same analysis presented for the dynamical intensity of cyclones has been repeated for the hydrological intensity, i.e. the area–averaged precipitation rate in a 5 degrees spherical cap centered on the cyclone. The FD of the along–track maxima in the cyclones hydrological intensity (Fig. 6c–d) shows a future reduction (RCP4.5-HIST) in the number of weakly precipitating cyclones and an increase in the number of strong and extreme precipitating cyclones in both DJF and JJA. In the multi–model mean, there is a $26 \pm 2\,\%$ (DJF) and

$33 \pm 2\,\%$ (JJA) increase in the number of cyclones with precipitation intensity within the top 10% of the HIST simulations. Fig. 7c shows that the response has the same sign in all the CMIP5 models, though the spread in the model responses appears to be large (10%–56% in DJF, 0%–60% in JJA). A larger mean signal and a larger spread of the responses are found for the RCP8.5 scenario.

b. Spatial distribution of the strong cyclones response

Fig. 8a shows the DJF mean track density response of the subset of cyclones associated with strong wind speeds which is defined in the previous subsection. Only the responses statistically significant at the 10% level are displayed. The DJF response is dominated by a large ($\sim 20\%$) track density reduction between Newfoundland and the Greenland sea. This signal contributes to the basin–wide reduction in the number of strong cyclones found in the previous subsection. However, we also note a smaller increase in the track density of strong cyclones between the British Isles and Scandinavia. In particular, the multi model mean shows a track density increase of $3 \pm 5\,\%$ by averaging the mean response over the same Central European area considered in section 3f.

To further analyse the increase in European storminess, Fig. 8c shows the mean response in the dynamical intensity of the subset of the strong cyclones. While no significant changes are found over most of the Atlantic, an increase in the 850 hPa wind speeds of the strong cyclones is found over Central Europe in the multi–model mean ($+3 \pm 1\,\%$). The increase in both the number and the dynamical intensity of the cyclones associated with strong wind speeds might contribute to larger economic loss potential due to cyclone activity (Mailier et al. 2006; Pinto et al. 2007a). However, the signal to noise of the European track density and intensity responses are small and CMIP5 models tend to agree that the response is small ($f^2 < 1$).

Fig. 8b,d show the same analysis but for JJA. The dominant track density signal is a reduction along the southern flank of the stormtrack and in particular over North America.

However, the track density increases in the Norwegian sea area. This dipolar structure is related to the larger uncertainty in the JJA response compared with DJF (see Fig. 7b). In some models the low latitude reduction dominates (e.g. MIROC–ESM), while in other models the high latitude increase dominates (e.g. MIROC5).

It is also of interest to note that the mean intensity of the strong cyclones generally shows no significant changes over most of the Atlantic in both DJF and JJA. This suggests it is the number of strong cyclones, rather their intensity, which is predominantly effected by the large scale changes in the baroclinicity of the atmosphere. These changes are discussed in the next section.

5. Relation to the large scale environment

The anthropogenic forcing will alter the state of the atmosphere, of the ocean and of the sea ice. These changes may all affect the behaviour of cyclones by modifying the baroclinicity of the atmosphere and the role of diabatic processes in cyclone development. Understanding the role of these physical drivers of change is important to gain confidence in climate model projections. However, care is needed when attributing the response in the behaviour of cyclones to a specific change in a component of the climate system, as the responses of the different components are interconnected. Here we investigate the consistency of the North Atlantic cyclone responses with the large scale changes in the baroclinicity of the atmosphere. In particular, we discuss why the reduction in strong cyclone activity mainly occurs along the northern flank of the stormtrack in DJF and on the southern flank in JJA.

Fig. 9a–b shows the mean climate response (RCP4.5-HIST) in the near surface atmospheric air temperature (T2m). The DJF response in T2m is dominated by the surface polar amplification of global warming which is related with the Arctic sea ice lost and radiative feedback processes (Holland and Bitz 2003). The low level meridional temperature gradient and atmospheric baroclinicity along the northern flank of the stormtrack are there-

fore reduced. This is consistent with the found reduction in the number of strong cyclones. Furthermore, a minimum in SST warming is found in the North Atlantic. Previous studies (Brayshaw et al. 2009; Woollings et al. 2012) suggested that this minimum in North Atlantic SST warming, which is associated with the weakening of the MOC, might influence the eastward extension of the stormtrack into Europe by enhancing the atmospheric baroclinicity in the East Atlantic. In JJA, the response in T2m has a more uniform spatial distribution and it shows very little polar amplification of global warming. This is consistent with the absence of a decrease in high latitude cyclone activity in JJA, in contrast to DJF.

Fig. 9c–d shows the mean response (RCP4.5-HIST) in the zonal wind at 250 hPa (U250). U250 gives the intensity of the jet stream and it is a measure of the atmospheric baroclinicity, via thermal wind balance. In DJF, the mean response of U250 is composed of strengthening on the subtropical side of the Atlantic jet stream and of an eastward extension into Europe. While the eastward extension of the jet appears to be consistent with the increase in European storminess, a reduction in the number of tracks is found in the Central Atlantic where the jet becomes stronger. This suggests that other mechanisms might be important in the region. Instead, the response in the jet stream and in the cyclone tracks are more closely associated in JJA. U250 decreases on the southern flank of the jet stream and increases on the northern flank (see Fig. 9d). The pattern is suggestive of a poleward shift and resembles the track density response.

A common feature of the DJF and JJA track density and dynamical intensity responses is a reduction on the southernmost latitudes with cyclone activity. This common feature is likely associated with the well known tendency to a *broadening of the tropics* and increase in subtropical static stability in response to climate change (Seidel et al. 2007; Lu et al. 2008, 2009).

6. Conclusions and discussion

In this study we have investigated the response of the winter (DJF) and summer (JJA) North Atlantic and European extratropical cyclones to climate change in the CMIP5 models. This is motivated by the large socio–economic impact that changes in the location and intensity of extratropical cyclones might have on Europe. The climate response is computed as a difference between thirty years periods of the HISTORICAL (1976–2005) and future day (2070–2099) simulations in the RCP4.5 and RCP8.5 emission scenarios. A cyclone tracking technique (Hodges 1994, 1999) is used to quantify the response in the number of cyclones and in their intensity, which is measured by the maximum windspeed at 850 hPa (dynamical intensity) and by the area averaged precipitation (hydrological intensity). In contrast to previous studies, that only looked at cyclone tracks in individual or small groups of models, the inspection of a large multi–model ensemble allows the uncertainties in the projection to be quantified (Sansom et al. 2012).

With regard to the response in the RCP4.5 scenario, the main results of this study are:

- In DJF, the response of North Atlantic and European cyclones is characterised by a tripolar pattern, rather than by a poleward shift. In the multi model mean, the number of cyclones decreases in the Norwegian sea, while a small, but significant, increase is found over the British Isles ($+3 \pm 2\,\%$)[2]. A larger reduction in the number of cyclones is found in the Mediterranean ($-12 \pm 2\,\%$). The total number of cyclones decreases ($-3.6 \pm 0.6\,\%$).

- In JJA there is a reduction in cyclone activity (number and intensity) along the southern flank of the North Atlantic stormtrack, which is associated with the poleward shift of the upper tropospheric jet. The total number of cyclones decreases ($-1.9 \pm 0.6\,\%$).

- The mean hydrological intensity of cyclones shows a large increase consistent with the warming of surface air temperature. North of 45N, and especially over land, the signal

[2]The values in brackets show the mean response and the 90% confidence interval due to internal variability

to noise is in the rage 4–6, which is large compared with the response in the number and dynamical intensity of cyclones.

- On a basin scale, the number of cyclones associated with the 90% percentiles strong wind speeds decreases. However, both the number ($+3 \pm 5\,\%$) and the mean wind speed ($+3 \pm 1\,\%$) of these strong cyclones increases over the UK and central Europe in DJF.

- Apart from the large Mediterranean response in DJF, the track density and dynamical intensity responses have signal to noise ratio of the order of one. This clearly indicates that using multiple runs of the present and future climate is needed to accurately quantify the response of extratropical cyclone in climate model simulations.

The same conclusions are drawn from the climate response to the RCP8.5 scenario, where both the mean response and the spread of the model responses tend to become larger.

There are multiple factors that contribute to the confidence in these multi–model projections. First, the mean response of the CMIP5 models appears to be qualitatively similar to some of those already presented in single model studies (Sinclair and Watterson 1999; Geng and Sugi 2003; Leckebusch and Ulbrich 2004; Pinto et al. 2007b; Bengtsson et al. 2006, 2009; Pinto et al. 2009; Catto et al. 2011). As some of these studies use a different tracking algorithm, the similarity suggests that the projections presented in this study are likely to be robust with respect to the employed methodology. Second, under the RCP4.5 forcing, we have found that the uncertainty in the track density and dynamical intensity projections due to differences in the responses of the models is smaller than the uncertainty due to natural variability. This is indicative of consensus among the CMIP5 model projections. Third, the tripolar pattern characterising the response of North Atlantic cyclones in DJF seems to be only weakly affected by the biases of the models in capturing the observed tilt and the position of the North Atlantic stormtrack. Finally, the response of the cyclones appears to be consistent with well known changes in the large scale environment such as the broadening

of the tropics, the polar amplification of global warming (DJF) and the poleward shift of the jet (JJA).

The ultimate source of confidence comes from detecting and attributing the changes predicted by the models in the observed cyclone statistics. This study identifies the responses that can be expected to emerge first from natural variability. The increase in the mid to high latitude hydrological intensity of cyclones over land has the largest signal to noise, followed by the reduction in the number of Mediterranean cyclones in DJF and by the reduction in cyclone activity along the southern flank of the Atlantic stormtrack in JJA. The signal to noise ratio in the responses of the number and dynamical intensity of North Atlantic cyclones in DJF appear to be small, which might make the detection of any change more difficult.

These results suggest that changes in North Atlantic and European cyclones may be important for adaptation planning to climate change. In particular, the increase in both the hydrological and dynamical intensity of cyclones can enhance the windstorm and flood risk over the British Isles and Central Europe. The large reduction in the number of Mediterranean cyclones in winter may affect the fresh water availability of the region, which is largely dependent on the storage of the cyclone generated wintertime precipitation. To increase confidence in these projections it would be useful to better understand their relation with the physical drivers of change. In particular, the sensitivity of cyclone behaviour to the tropical SST warming, the North Atlantic SST warming, the weakening of the MOC and the Arctic sea ice lost will be investigated in future research.

Acknowledgments.

We acknowledge the World Climate Research Programme's Working Group on Coupled Modelling, which is responsible for CMIP, and we thank the climate modelling groups (listed in Table 1 of this paper) for producing and making available their model output. For CMIP the U.S. Department of Energy's Program for Climate Model Diagnosis and Intercomparison provides coordinating support and led development of software infrastructure in partnership

539 with the Global Organisation for Earth System Science Portals. This research has been
540 done under the Testing and Evaluating Model Projections of European STorms (TEMPEST)
541 project which is founded by the Natural and Environmental Research Council. GZ would
542 like to thank R. Lee for the help in retrieving some of the CMIP5 data.

APPENDIX

a. The ANOVA framework

Let y_{msr} represent a climate statistic from model m, scenario s and run r from a multi model ensemble of M models and N runs containing an historical (H) and a future (F) scenario. Sansom et al. (2012) show that y_{msr} can be described by the ANOVA framework:

$$\begin{aligned} y_{msr} &= \mu + \alpha_m + \beta_s + \gamma_{ms} + \epsilon_{msr} \\ \epsilon_{msr} &\overset{iid}{\sim} N\left(0, \sigma^2\right), \end{aligned} \tag{A1}$$

where the effect μ is the expected climate in the historical scenario and β_F is the expected climate change response. The effect α_m is the difference between the historical climate of model m and the expected climate μ. The interaction terms γ_{mF} represent the difference between the climate response simulated by model m and the expected response β_F. The random component ϵ_{msr} represents the internal variability in the y_{msr} and is assumed to be normally distributed. The framework is subject to the constraints that $\sum_{m=1}^{M} \alpha_m = 0$, $\beta_H = 0$, $\gamma_{mH} = 0$ for all models and $\sum_{m=1}^{M} \gamma_{mF} = 0$.

b. Mean climate response

The maximum-likelihood (ML) estimate ($\hat{\beta}_F$) of the expected climate response β_F is:

$$\hat{\beta}_F = \frac{1}{M} \sum_{m=1}^{M} \left(\overline{y}_{mF.} - \overline{y}_{mH.}\right) \tag{A2}$$

where R_{ms} is the number of runs of model m in scenario s and $\overline{y}_{ms}$ is the average of y_{msr} over the multiple runs. $\hat{\beta}_F$ is equivalent to the "*one model, one vote*" multi–model mean approach of the climate response estimate.

The estimated variance of β_F is

$$Var\left(\hat{\beta}_F\right) = \frac{\hat{\sigma}^2}{M^2} \sum_{m=1}^{M} \left(\frac{R_{mH} + R_{mF}}{R_{mH} R_{mF}}\right) \tag{A3}$$

$$\hat{\sigma}^2 = \frac{1}{N - 2M} \sum_{m=1}^{M} \sum_{s \in \{H,F\}} \sum_{r=1}^{R_{ms}} \left(y_{msr} - \overline{y}_{ms.}\right)^2, \tag{A4}$$

where $\hat{\sigma}^2$ is the ML estimate of the internal variability. The signal to noise ratio is defined as $\hat{\beta}_F/\hat{\sigma}$. Only for the hydrological intensity, due to data limitation, σ is computed from the HIST runs only. See Sansom et al. (2012) for full details of the estimation procedure.

The hypothesis of a non-zero climate response ($H_a : \beta_F \neq 0$) can be tested by comparing the test statistic

$$T_\beta = \frac{|\hat{\beta}_F - 0|}{\sqrt{Var\left(\hat{\beta}_F\right)}}, \tag{A5}$$

with the quantiles of the t-distribution with $N - 2M$ degrees of freedom.

The relative amplitude of the mean climate response ($r = \hat{\beta}_F/\hat{\mu}$) has variance $Var(r) \sim Var(\hat{\beta}_F)/\hat{\mu}$, where $\hat{\mu}$ is the multi–model mean historical climate. The uncertainty on μ has been neglected as small compared to the one on $\hat{\beta}_F$.

c. Variance ratio f^2

The variance ratio f^2 is a useful measure of agreement between models on the climate change response. It is the ratio of the variance explained by the model–dependance in the climate change response (γ_{mF} interaction terms) compared to the variance explained by the internal variability. The fraction of variance explained by internal variability is given by $1-R^2_\gamma$, where R^2_γ is the coefficient of determination of the ANOVA framework. The coefficient of determination gives the proportion of the total variability explained by the framework. The fraction of variance explained by the model–dependent component is obtained as the difference between the variance explained by the ANOVA framework above (R^2_γ) and the variance explained by a simpler framework (R^2_α) where the interaction terms are constrained to be zero ($\gamma_{mF} = 0 \ \forall \ m$). Therefore, $f^2 = (R^2_\gamma - R^2_\alpha)/(1 - R^2_\gamma)$. See Sansom et al. (2012) for a detailed description of the simpler framework.

REFERENCES

Bengtsson, L., K. I. Hodges, and N. Keenlyside, 2009: Will extratropical storms intensify in a warmer climate? *J. Climate*, **22**, 2276–2301.

Bengtsson, L., K. I. Hodges, and E. Roeckner, 2006: Storm tracks and climate change. *J. Climate*, **19**, 3518–3543.

Blender, R. and M. Schubert, 2000: Cyclone tracking in different spatial and temporal resolutions. *Mon Wea Rev*, **128**, 377–384.

Brayshaw, D. J., T. Woollings, and M. Vellinga, 2009: Tropical and Extratropical Responses of the North Atlantic Atmospheric Circulation to a Sustained Weakening of the MOC. *Journal of Climate*, **22**, 3146–3155.

Catto, J., L. Shaffrey, and K. Hodges, 2011: Northern Hemisphere extratropical cyclones in a warming climate in the HiGEM high resolution climate model. *J. Climate*, **24**, 5336–5352.

Della-Marta, P. M. and J. G. Pinto, 2009: Statistical uncertainty of changes in winter storms over the North Atlantic and Europe in an ensemble of transient climate simulations. *Geophys. Res. Lett*, **36**, L14 703.

Emori, S. and S. J. Brown, 2005: Dynamic and thermodynamic changes in mean and extreme precipitation under changed climate. *Geophys. Res. Lett*, **32**, L17 706.

Finnis, J., M. Holland, M. Serreze, and J. Cassano, 2007: Response of Northern Hemisphere extratropical cyclone activity and associated precipitation to climate change, as represented by the Community Climate System Model. *J. Geophys. Res*, **112**, G04S42.

Fu, Q., C. M. Johanson, J. M. Wallace, and T. Reichler, 2006: Enhanced Mid-Latitude Tropospheric Warming in Satellite Measurements. *Science*, **312**, 1179–1179.

611 Geng, Q. and M. Sugi, 2003: Possible change of extratropical cyclone activity due to en-
612 hanced greenhouse gases and sulfate aerosols-study with a high-resolution AGCM. *J. Cli-*
613 *mate*, **16**, 2262–2274.

614 Harvey, B. J., L. C. Shaffrey, T. J. Woollings, G. Zappa, and K. I. Hodges, 2012: How large
615 are projected 21st century storm track changes? *Geophys. Res. Lett*, **Submitted**.

616 Hawcroft, M. K., L. C. Shaffrey, and H. F. Dacre, 2012: How important is the contribution
617 of extratropical cyclones to Northern Hemisphere precipitation? *Geophys. Res. Lett*, **In**
618 **preparation**.

619 Held, I., 1993: Large-scale dynamics and global warming. *B Am Meteorol Soc*, **74**, 228–241.

620 Held, I. and B. Soden, 2006: Robust responses of the hydrological cycle to global warming.
621 *J. Climate*, **19**, 5686–5699.

622 Hodges, K., 1999: Adaptive constraints for feature tracking. *Mon Wea Rev*, **127**, 1362–1373.

623 Hodges, K. I., 1994: A general method for tracking analysis and its application to meteoro-
624 logical data. *Mon Wea Rev*, **122**, 2573–2586.

625 Hodges, K. I., 1995: Feature Tracking on the Unit Sphere. *Mon Wea Rev*, **123**, 3458–3465.

626 Hodges, K. I., 1996: Spherical nonparametric estimators applied to the UGAMP model
627 integration for AMIP. *Mon Wea Rev*, **124**, 2914–2932.

628 Holland, M. M. and C. M. Bitz, 2003: Polar amplification of climate change in coupled
629 models. *Clim Dyn*, **21**, 221–232.

630 Hoskins, B. and P. Valdes, 1990: On the existence of storm-tracks. *J. Atmos. Sci*, **47**, 1854–
631 1864.

632 Hwang, Y., D. Frierson, and J. Kay, 2011: Coupling between Arctic feedbacks and changes
633 in poleward energy transport. *Geophys. Res. Lett*, **38**, L17 704.

Laîné, A., M. Kageyama, D. Salas-Mélia, G. Ramstein, S. Planton, S. Denvil, and S. Tyteca, 2009: An Energetics Study of Wintertime Northern Hemisphere Storm Tracks under 4 CO2 Conditions in Two Ocean-Atmosphere Coupled Models. *J. Climate*, **22**, 819–839.

Lambert, S. J. and J. C. Fyfe, 2006: Changes in winter cyclone frequencies and strengths simulated in enhanced greenhouse warming experiments: results from the models participating in the IPCC diagnostic exercise. *Clim Dyn*, **26 (7)**, 713–728.

Leckebusch, G. C. and U. Ulbrich, 2004: On the relationship between cyclones and extreme windstorm events over Europe under climate change. *Global Planet Change*, **44**, 181–193.

Lionello, P. and F. Giorgi, 2007: Winter precipitation and cyclones in the Mediterranean region: future climate scenarios in a regional simulation. *Adv. Geosci.*, **12**, 153–158.

Lu, J., G. Chen, and D. M. W. Frierson, 2008: Response of the Zonal Mean Atmospheric Circulation to El Niño versus Global Warming. *J. Climate*, **21 (22)**, 5835–5851.

Lu, J., C. Deser, and T. Reichler, 2009: Cause of the widening of the tropical belt since 1958. *Geophysical Research Letters*, **36**, L03 803.

Mailier, P., D. Stephenson, C. Ferro, and K. I. Hodges, 2006: Serial clustering of extratropical cyclones. *Monthly Weather Review*, **134 (8)**, 2224–2240.

Meehl, G., et al., 2007: *Global Climate Projections. In: Climate Change 2007: The Physical Science Basis. Contribution of Working Group I to the Fourth Assessment Report of the Intergovernmental Panel on Climate Change Edited by: [S Solomon, D Qin, M Manning, Z Chen, M Marquis, K.B. Averyt, M Tignor, and H.L. Miller (eds.)]*. Cambridge University Press, Cambridge.

Meinshausen, M., et al., 2011: The RCP greenhouse gas concentrations and their extensions from 1765 to 2300. *Climatic Change*, **109**, 213–241, doi:10.1007/s10584-011-0156-z.

O'Gorman, P. A., 2010: Understanding the varied response of the extratropical storm tracks to climate change. *P Natl Acad Sci*, **107**, 19 176–19 180.

Pall, P., M. R. Allen, and D. A. Stone, 2007: Testing the Clausius–Clapeyron constraint on changes in extreme precipitation under CO2 warming. *Clim Dyn*, **28**, 351–363.

Pinto, J., E. Fröhlich, G. Leckebusch, and U. Ulbrich, 2007a: Changing European storm loss potentials under modified climate conditions according to ensemble simulations of the ECHAM5/MPI-OM1 GCM. *Nat. Hazards Earth Syst. Sci*, **7**, 165–175.

Pinto, J., T. Spangehl, A. Fink, G. C. Leckebusch, and U. Ulbrich, 2009: Factors Contributing to the Development of Extreme North Atlantic Cyclones and Their Relationship with the NAO. *Clim Dyn*, **32**, 711–737.

Pinto, J., U. Ulbrich, G. Leckebusch, T. Spangehl, M. Reyers, and S. Zacharias, 2007b: Changes in storm track and cyclone activity in three SRES ensemble experiments with the ECHAM5/MPI-OM1 GCM. *Climate Dynamics*, **29**, 195–210.

Raible, C. C., B. Ziv, H. Saaroni, and M. Wild, 2010: Winter synoptic-scale variability over the Mediterranean Basin under future climate conditions as simulated by the ECHAM5. *Clim Dyn*, **35**, 473–488.

Sansom, P., C. Ferro, G. Zappa, L. Shaffrey, and D. Stephenson, 2012: A simple framework for weighting climate change projections in multi-model ensembles. *J. Climate*, **Submitted**.

Schneider, T., P. O'Gorman, and X. Levin, 2010: Water vapor and the dynamics of climate changes. *Rev. Geophys*, **48**, RG3001.

Schneidereit, A., R. Blender, and K. Fraedrich, 2010: A radius–depth model for midlatitude cyclones in reanalysis data and simulations. *Q J Roy Meteor Soc*, **136**, 50–60.

Schubert, M., J. Perlwitz, R. Blender, and K. Fraedrich, 1998: North Atlantic cyclones in CO2-induced warm climate simulations: Frequency, intensity, and tracks. *Clim Dyn*, **14**, 827–837.

Seidel, D. J., Q. Fu, W. J. Randel, and T. J. Reichler, 2007: Widening of the tropical belt in a changing climate. *Nature Geoscience*, **1**, 21–24.

Sinclair, M. and I. Watterson, 1999: Objective assessment of extratropical weather systems in simulated climates. *J. Climate*, **12**, 3467–3485.

Taylor, K., R. Stouffer, and G. Meehl, 2012: An overview of CMIP5 and the experiment design. *Bull.Amer.Meteor.Soc*, **93**, 485–498.

Ulbrich, U., G. Leckebusch, and J. Pinto, 2009: Extra-tropical cyclones in the present and future climate: a review. *Theor Appl Climatol*, **96**, 117–131.

Ulbrich, U., J. G. Pinto, H. Kupfer, G. C. Leckebusch, T. Spangehl, and M. Reyers, 2008: Changing Northern Hemisphere Storm Tracks in an Ensemble of IPCC Climate Change Simulations. *J. Climate*, **21**, 1669–1679.

Woollings, T., 2010: Dynamical influences on European climate: an uncertain future. *Phil. Trans. R. Soc. A*, **368**, 3733–3756.

Woollings, T., J. M. Gregory, J. G. Pinto, M. Reyers, and D. J. Brayshaw, 2012: Response of the North Atlantic storm track to climate change shaped by ocean–atmosphere coupling. *Nature Geoscience*, **5**, 313–317.

Yin, J., 2005: A consistent poleward shift of the storm tracks in simulations of 21st century climate. *Geophys. Res. Lett*, **32**, L18 701.

Zappa, G., L. Shaffrey, and K. Hodges, 2012: The ability of CMIP5 models to simulate North Atlantic extratropical cyclones. *J. Climate*, **Submitted**.

List of Tables

	Basic Information		Atm. Resolution		Num. runs.		Precip
	Model Name	Institution	Horizontal	Vertical	HIST	RCP	y/n
1	HadGEM2-ES	MOHC,*UK*	N96 (192x144)	38	1	1	n
2	HadGEM2-CC		N96 (192x144)	38	2	1	n
3	INMCM4	INM, *Russia*	180x120	21	1	1	y
4	CanESM2	CCCma, *Canada*	T42 (128x64)	35	1	1	n
5	IPSL-CM5A-LR	IPSL,*France*	96x95	39	5	4	y
6	IPSL-CM5A-MR		144x142	39	1	1	y
7	CNRM-CM5	CNRM, *France*	T84 (256x128)	31	5	1	y[1]
8	BCC-CSM1-1	BCC, *China*	T42 (128 x64)	26	3	1	y
9	NorESM1-M	NCC, *Norway*	144x96	26	3	1	y
10	CSIRO-Mk3.6.0	CSIRO, *Australia*	T63 (192x96)	18	5	5	n
11	EC-EARTH	SMHI/MISU, *Europe*	TL159 (320x160)	62	3	3	y
12	MRI-CGCM	MRI, *Japan*	TL159 (320x160)	48	5	1	n
13	MPI-ESM-LR	MPI–M, *Germany*	T63 (192x96)	47	3	3	n
14	MIROC5	MIROC,*Japan*	T63 (192x96)	56	1	1	y
15	MIROC-ESM		T42 (128x64)	80	3	1	y
16	MIROC-ESM-CHEM		T42 (128x64)	80	3	1	y
17	GFDL-ESM2M	GFDL,*USA*	144x90	24	1	1	y
18	GFDL-ESM2G		144x90	24	1	1	y
19	FGOALS-g2	LASG,*CHINA*	128x60	26	1	1	y

TABLE 1. List of CMIP5 models considered in the study. For each model the following features are described: the resolution of the atmospheric component, the number of HISTORICAL (HIST) and RCP4.5/RCP8.5 (RCP) runs, the availability of high frequency precipitation data. (1) Precipitation is available for only one HIST run.

		EU DJF		EU JJA		MED DJF	
		$r(\%)$	β/σ	$r(\%)$	β/σ	$r(\%)$	β/σ
Tden	RCP4.5	2±1	0.7	-4±2	1.2	-12±2	2.9
	RCP8.5	4±1	1.1	-10±2	2.5	-20±2	4.8
Wind	RCP4.5	0.4±0.5	0.3	-1.4±0.5	1.2	-1.8±0.5	1.6
	RCP8.5	0.9±0.5	0.8	-0.3±0.5	0.2	-3.0±0.5	2.5
Precip	RCP4.5	9±1	7	8±1	3.5	3±1	1.5
	RCP8.5	18±1	14	9±1	3.8	0±1	0.1

TABLE 2. Area averaged multi–model mean response for the RCP4.5 and RCP8.5 emission scenarios in the central European area (DJF and JJA) and for the Mediterranean area (DJF). The investigated fields are the track density (Tden), dynamical cyclone intensity (Wind) and the hydrological cyclone intensity (Precip). r(%) is the mean response (β) expressed as percentage change on the mean HIST values. The 90% confidence intervals on r due to internal variability are indicated (see the Appendix for details on the estimation procedure). β/σ is the signal to noise ratio.

List of Figures

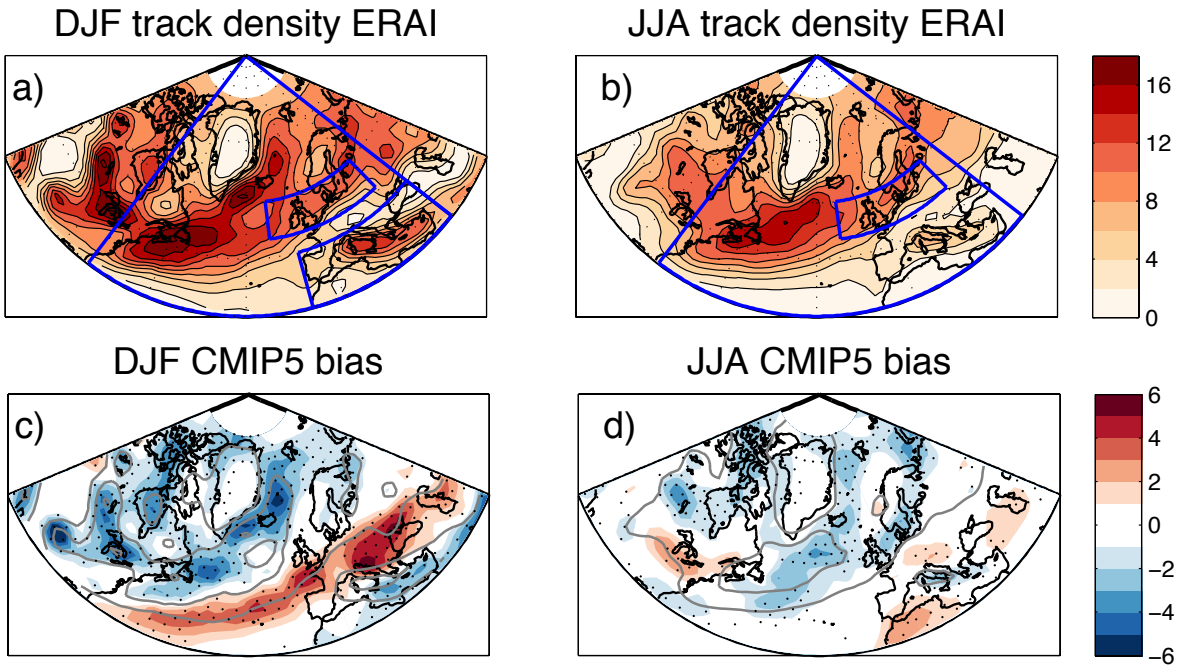

FIG. 1. Track density in ERA–Interim reanalysis (1980–2009) (a–b) and mean track density bias of CMIP5 models in the HIST simulations relative to ERA–Interim (c–d). The results are shown for DJF (a,c) and JJA (b,d). Unites are in number of cyclones per month per unit area, where unit area is equivalent to a 5 degree spherical cap. Stippling shows are where more than 80% of the models have a bias of the same sign. In a–b the circular sector defines the region of the North Atlantic and European cyclones. The small *boxes* define the Mediterranean (DJF only) and Central European area of interests.

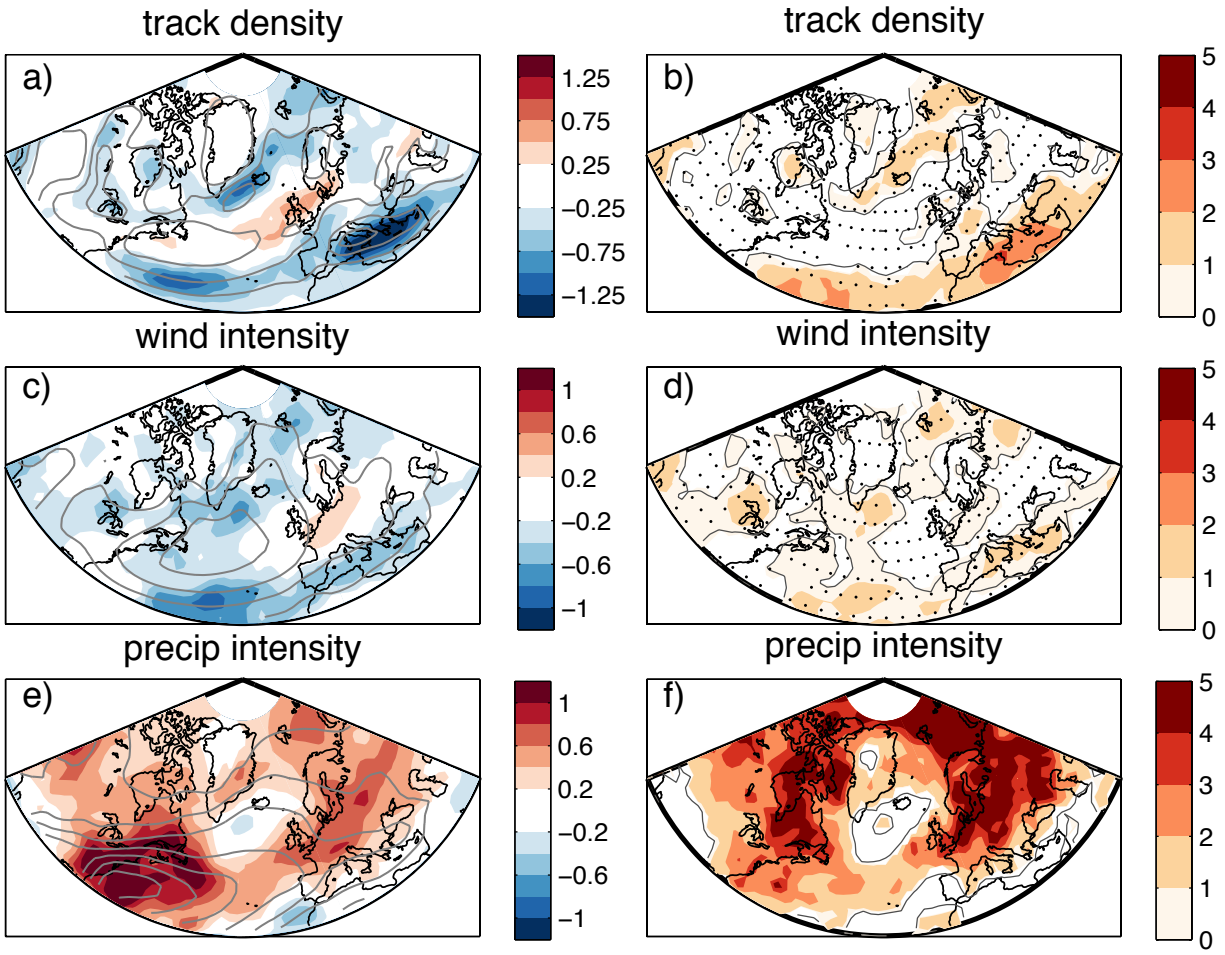

FIG. 2. DJF multi-model mean response (left panels) and statistical analysis (right panels) of the (a–b) track density, (c–d) mean cyclone intensity measured by 850 hPa wind speed and (e–f) mean precipitation intensity. In the left panels the grey contours show the multi model mean values in the HISTORICAL simulations with c.i. of (a) 4 number of cyclones per month per unit area, (c) 4 $\mathrm{m\,s^{-1}}$ and (e) 2 $\mathrm{mm\,day^{-1}}$. The right panels show the signal to noise ratio (β/s) in the regions where the mean climate response is statistically significant at the 5% level. Stippling is applied where $f^2 < 1$ to show regions of consensus on the size of the responses (a,b,c,d only).

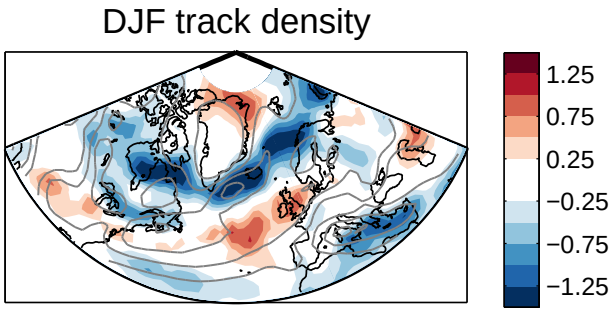

FIG. 3. DJF mean track density response (RCP4.5 - HIST) computed for only the 4 models with the best representation of the location and tilt of the North Atlantic stormtrack in CMIP5. Units are in number of cyclones per month per unit area.

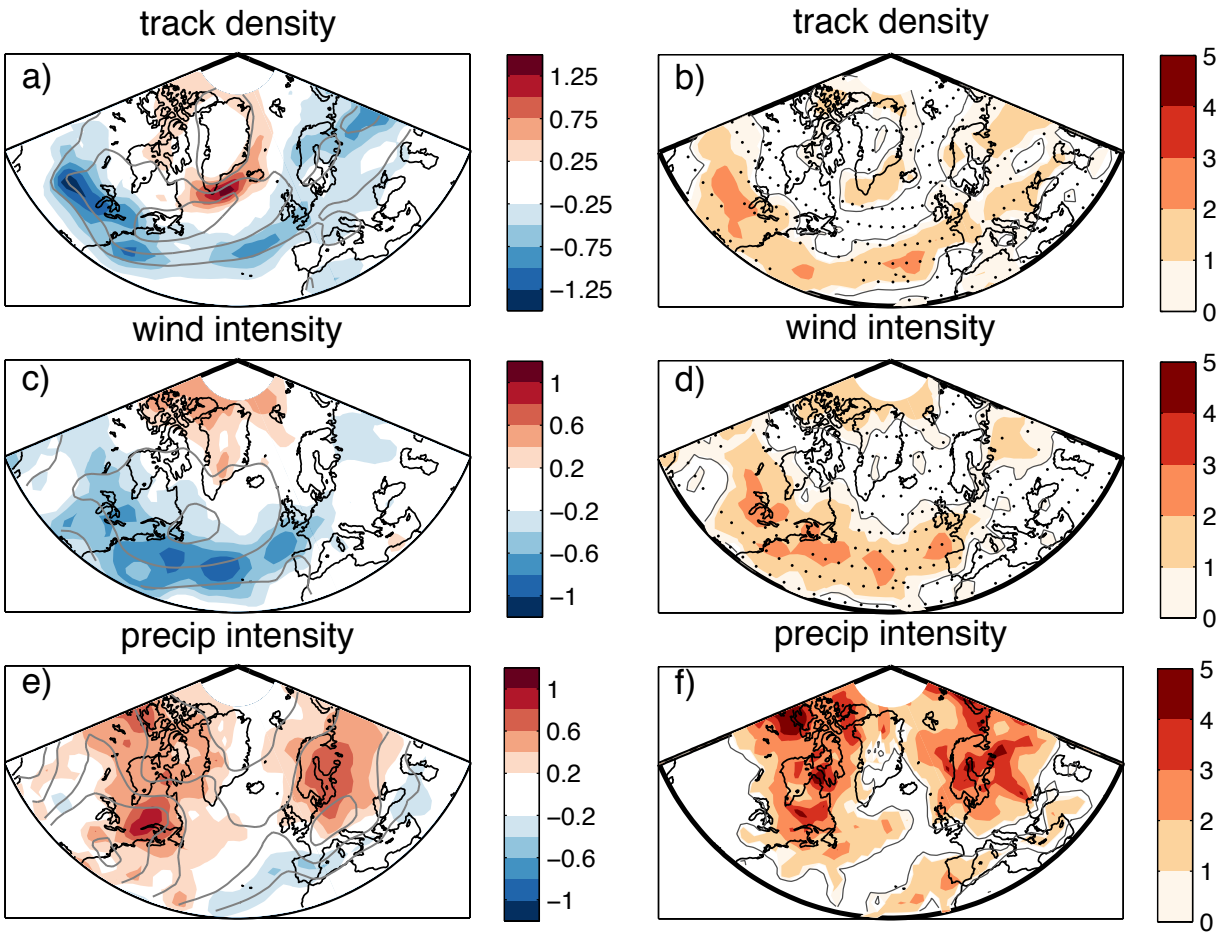

FIG. 4. Same as in fig. 2 but for JJA.

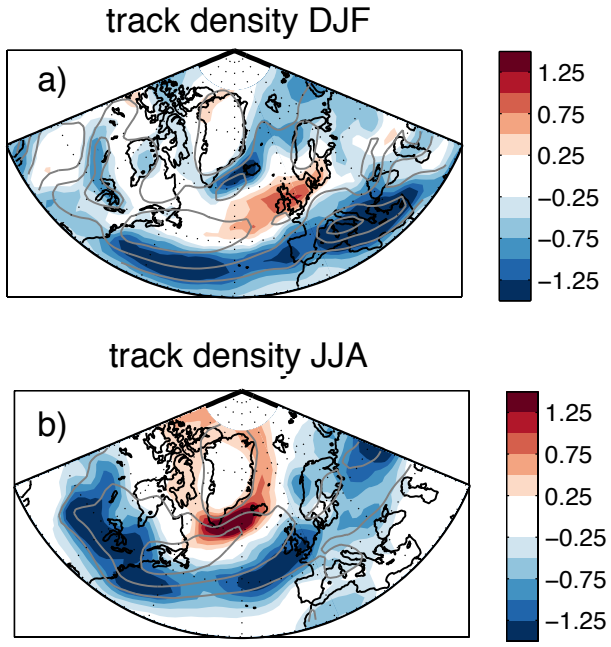

FIG. 5. As in Fig. 2a and Fig. 4a but for the track density response to the RCP8.5 scenario in DJF (top) and JJA (bottom). Units are in number of cyclones per month per unit area.

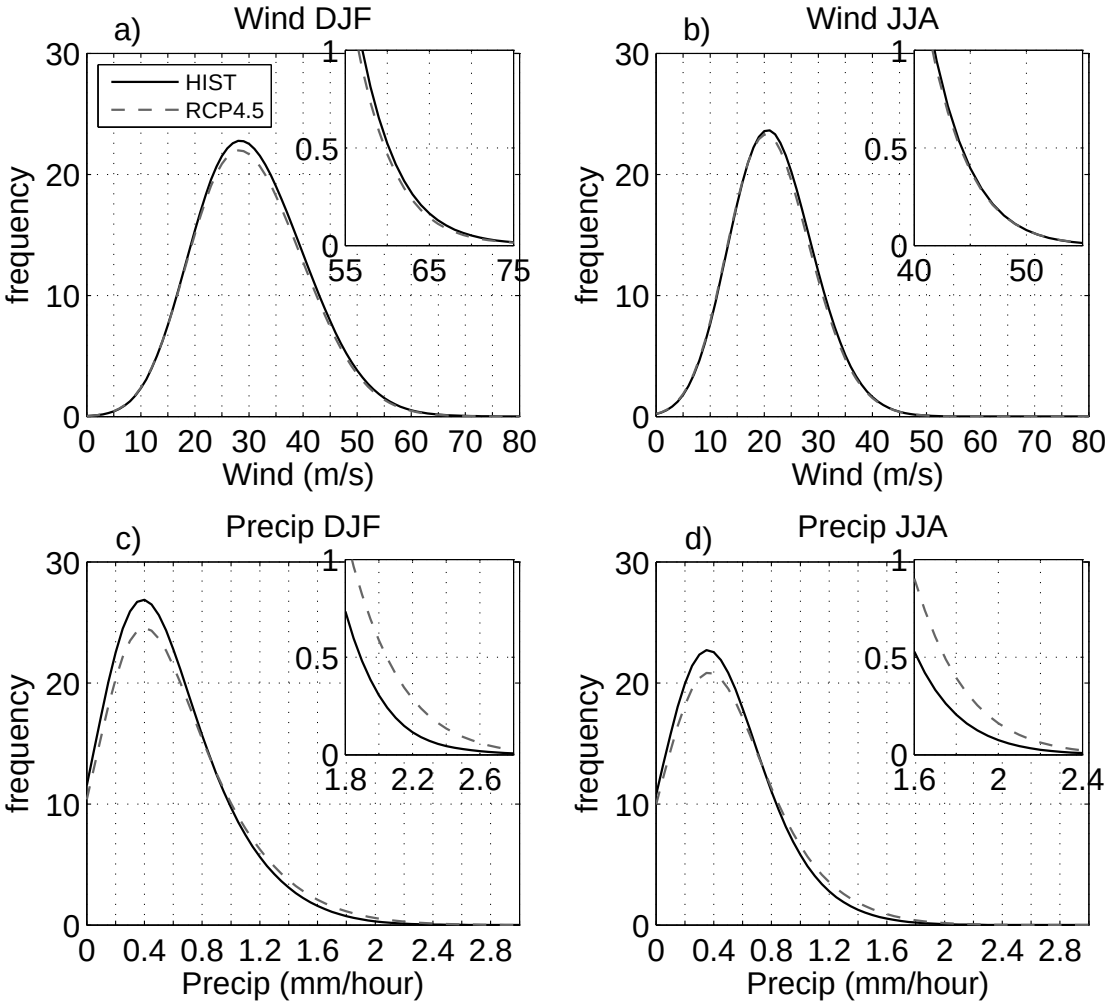

FIG. 6. Multi model mean of the frequency distributions of the maximum along–track wind speed (a,b) and precipitation (c,d) of North Atlantic and European cyclones. This is presented for DJF (a,c) and JJA (b,d). The full black line refers to the HIST simulation, and the dashed grey line to the RCP4.5 simulation. The frequency distribution of wind (precipitation) is scaled to number of cyclones per season per 5 $\mathrm{m\,s^{-1}}$ (0.2 $\mathrm{mm\,hour^{-1}}$)

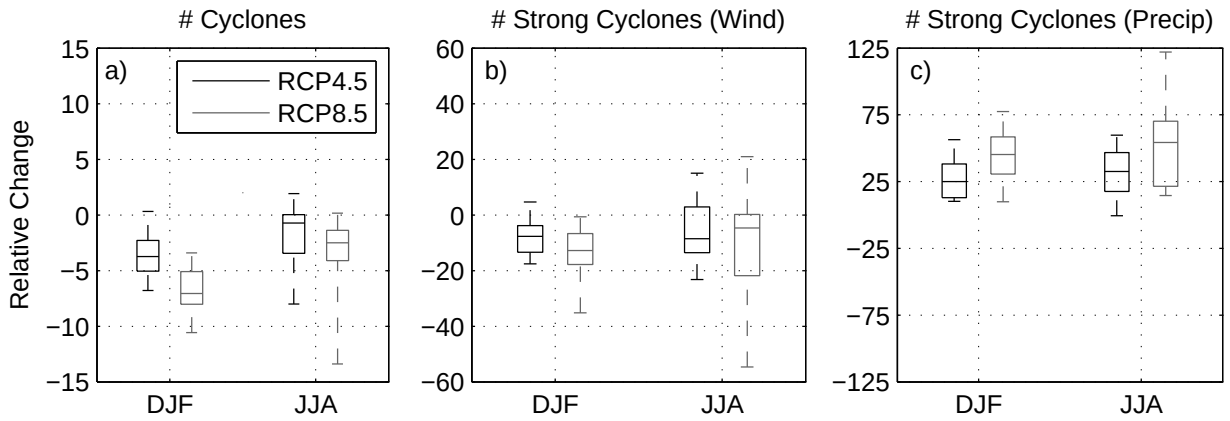

FIG. 7. Boxplot of the distribution of the model responses in the total number of cyclones (a), of the number of cyclones associated with strong winds (b) and with strong precipitation (c). The responses are expressed as relative changes relative to the HIST simulations. The centre of the box is the median response, the edges of the box extend to the 25–75 percentiles and the whiskers extend to the minimum and maximum values. Strong cyclones are defined as in text.

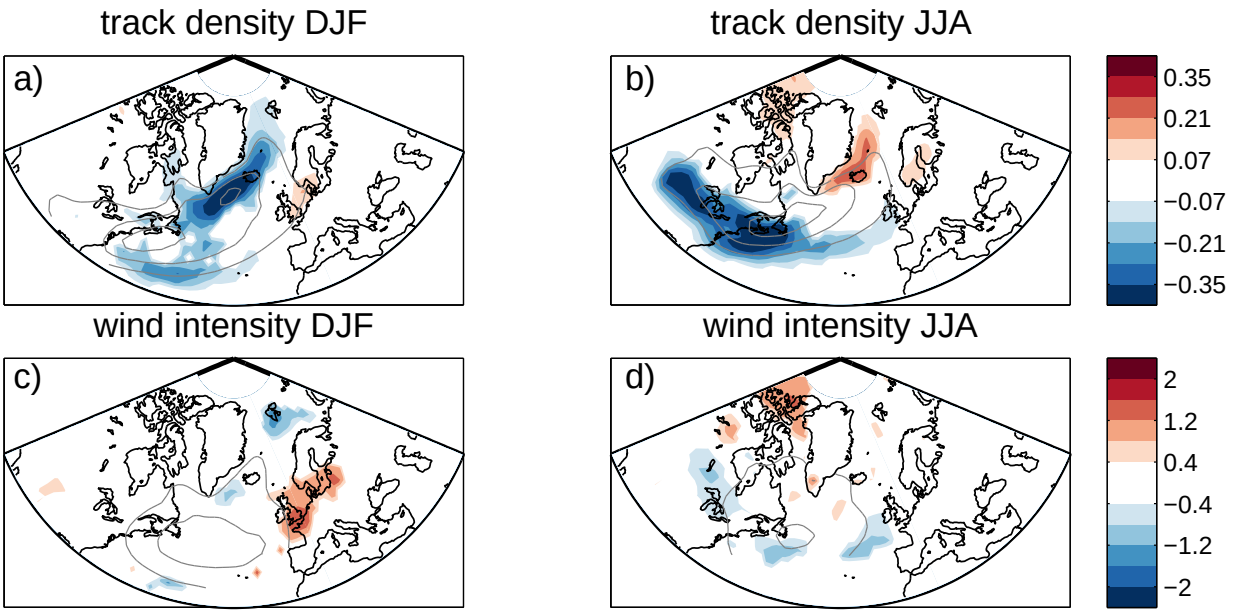

FIG. 8. Multi model mean track density (a–b) and dynamical intensity (c–d) responses (RCP4.5-HIST) computed for the subset of strong cyclones. The analysis is presented for DJF (a,c) and JJA (b,d). Strong cyclones are defined as in text. Only the responses statistically significant at the 10% level are displayed. The contours show the multi model mean values in the HIST simulations. In a) and in b) c.i. is 1 cyclones per month per unit area. In c) the selected contours are 30 $\mathrm{m\,s^{-1}}$ and 35 $\mathrm{m\,s^{-1}}$ while in d) are 20 $\mathrm{m\,s^{-1}}$ and 25 $\mathrm{m\,s^{-1}}$.

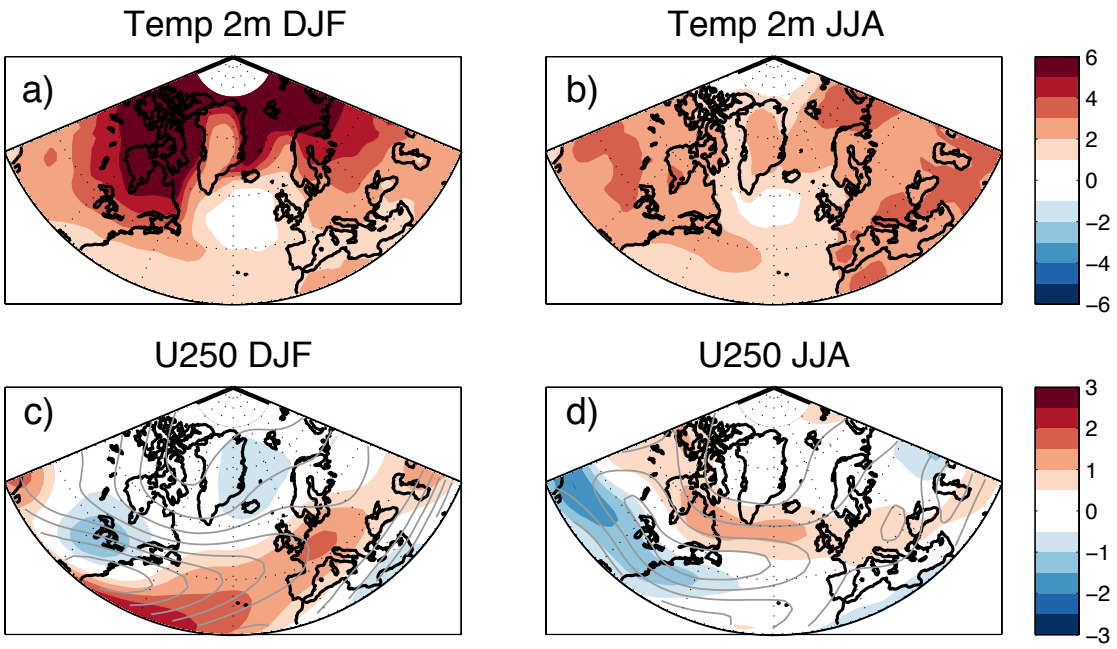

FIG. 9. Multi model mean response (RCP4.5 - HIST) in the near surface atmospheric air temperature (a–b) and in the zonal wind at 250 hPa (c–d). The responses are shown for DJF (a,c) and JJA (b,d). Units are C° in a–b and $\mathrm{m\,s^{-1}}$ in c–d. The mean values in the HIST simulations are displayed as contours in c–d with c.i. of 5 $\mathrm{m\,s^{-1}}$